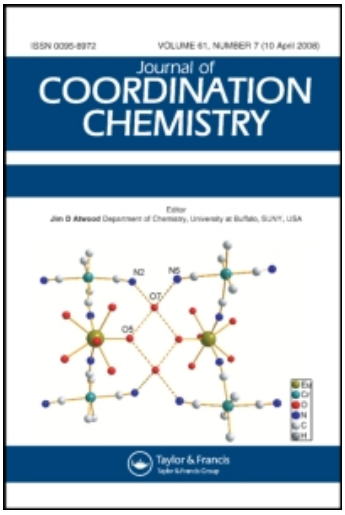

Journal of Coordination Chemistry
Publication details, including instructions for authors and subscription information:
http://www.informaworld.com/smpp/title~content=t713455674

CALORIMETRIC STUDY OF THERMOCHROMIC COMPLEXES. 2. HEAT CAPACITY AND PHASE TRANSITION OF BIS(*N,N*-DIETHYLETHYLENEDIAMINE)COPPER(II) PERCHLORATE

Akihito Nishimori[a]; Michio Sorai[a]; Edward A. Schmitt[b]; David N. Hendrickson[b]
[a] Microcalorimetry Research Center, Faculty of Science, Osaka University, Toyonaka, Osaka, Japan [b] Department of Chemistry, University of California at San Diego, La Jolla, California, USA

To cite this Article Nishimori, Akihito , Sorai, Michio , Schmitt, Edward A. and Hendrickson, David N.(1996) 'CALORIMETRIC STUDY OF THERMOCHROMIC COMPLEXES. 2. HEAT CAPACITY AND PHASE TRANSITION OF BIS(*N,N*-DIETHYLETHYLENEDIAMINE)COPPER(II) PERCHLORATE', Journal of Coordination Chemistry, 37: 1, 327 — 340
To link to this Article: DOI: 10.1080/00958979608023563
URL: http://dx.doi.org/10.1080/00958979608023563

J. Coord. Chem., 1996, Vol 37, pp. 327–340
Reprints available directly from the publisher
Photocopying permitted by license only

CALORIMETRIC STUDY OF THERMOCHROMIC COMPLEXES. 2. HEAT CAPACITY AND PHASE TRANSITION OF BIS(*N,N*-DIETHYLETHYLENEDIAMINE)COPPER(II) PERCHLORATE†

AKIHITO NISHIMORI, MICHIO SORAI*

Microcalorimetry Research Center, Faculty of Science, Osaka University, Toyonaka, Osaka 560, Japan

EDWARD A. SCHMITT and DAVID N. HENDRICKSON

Department of Chemistry, University of California at San Diego, La Jolla, California 92093-0358, USA

(Received November 30, 1994; in final form December 30, 1994)

The thermochromic phase transition of bis(*N,N*-diethylethylenediamine) copper(II) perchlorate has been studied by adiabatic calorimetry in the 12–359 K temperature range. A large heat capacity anomaly was observed at 317.64 K with a long heat-capacity tail extending down to ~200 K. The enthalpy and entropy of the phase transition were found to be $\Delta_{trs}H$ = 17.43 kJ mol^{-1} and $\Delta_{trs}S$ = 55.21 J K^{-1} mol^{-1}, respectively. Together with a calorimetric study of a homologous thermochromic complex, bis(*N,N*-diethylethylenediamine)copper(II) tetrafluoroborate (*J. Phys. Chem. Solids*, **55**, 99 (1994)), the nature of the present thermochromic phase transition is well described by a puckering motion of the copper-ligand chelate rings and a change in the ligand-field strength estimated on the basis of the angular overlap model. The correlation between structures, electronic spectra and thermal properties is discussed.

KEYWORDS: thermochromism, copper(II) complex, phase transition, heat capacity, puckering motion, angular overlap model

INTRODUCTION

A number of substances are known to be thermochromic.[1] There are many types of thermochromism; it can be reversible or irreversible, continuous or discontinuous, and can occur either in the solid state or in solution. The series $[M(dieten)_2]X_2$, where M is Cu^{2+} or Ni^{2+}, dieten is *N,N*-diethylethylenediamine, and X is BF_4^- or ClO_4^-, has been particularly well-studied.[2] They show a remarkable color change

†Contribution No. 98 from the Microcalorimetry Research Center. This paper is dedicated to Professor T. Iwamoto of the University of Tokyo. Part 1 of this series has been published in *J. Phys. Chem. Solids*, **55**, 99 (1994).

* Author for correspondence.

when they undergo phase transitions in the solid state. Thermochromism in $[Cu(dieten)_2](ClO_4)_2$ was first reported in 1938 by Pfeiffer *et al.*[3] The color of the copper complexes changes from red to blue-violet upon heating, while the color of the similar nickel complexes changes from orange to red. Both color changes are reversible. Infrared,[4] far-infrared,[4] electronic spectra,[4,5] magnetic measurement,[5] ESR,[5] differential scanning calorimetry (DSC),[6] X-ray diffraction[7,8] and NMR[8,9] have been reported. It was initially thought that the thermochromism was caused by axial approach of the anions to the copper or nickel ion.[5,6] However, when the crystal structures of both the low- and high-temperature phases were determined,[7,8] that idea turned out to be wrong. There exists no axial coordination of the counter anions in either of the phases because the bulky alkyl groups bonded to the nitrogen atoms prevent the counter anions from approaching the central metal atom. A new mechanism of thermochromism was proposed as follows: in the high-temperature phase the chelate rings pucker up and down while they remain static in the low-temperature phase. Such ring motion affects the ligand field strength, leading to the color change. This mechanism seems to be consistent with various experimental results so far available. However, the relationship between the microscopic aspects hitherto reported and the macroscopic energetic and entropic aspects is still unclear.

In a recent paper,[10] we reported the results of a calorimetric study of the phase transition of $[Cu(dieten)_2](BF_4)_2$. Precision heat capacity measurements were carried out with an adiabatic aclorimeter and a large heat-capacity anomaly associated with the color change was observed. The experimental results were interpreted on the basis of the Chesnut exciton model.[11] The thermodynamic quantities (ΔC_p, $\Delta_{trs}H$ and $\Delta_{trs}S$) were well reproduced by this model.

In order to gain more quantitative insight into the thermochromic mechanism of the series of complexes, in the present paper we estimate the difference of ligand-field energies between the low- and high-temperature phases on the basis of the angular overlap model and correlate it to the calorimetric results. In this paper we shall also discuss the thermal properties of $[Cu(dieten)_2](ClO_4)_2$ and compare them with those of $[Cu(dieten)_2](BF_4)_2$.

EXPERIMENTAL

Preparation of the Complex

The complex $[Cu(dieten)_2](ClO_4)_2$ was prepared according to the method described by Lever *et al.*[5] The elemental analysis for the complex gave a good agreement with the calculated values. *Anal.* Calcd. for $C_{12}H_{32}N_4CuCl_2O_8$(%): C, 29.13; H, 6.52; N, 11.32. Found: C, 28.95; H, 6.52; N, 11.24.

Differential Thermal Analysis (DTA)

The qualitative nature of the thermal properties of $[Cu(dieten)_2](ClO_4)_2$ was examined by use of a home-built DTA apparatus in the 100–380 K range.

Heat Capacity Measurements

Heat capacity measurements were carried out with an adiabatic calorimeter[12,13] in the 12–359 K range. The mass of sample loaded in a calorimeter cell made of gold

and platinum was 10.0294 g (0.0202672 mol). The mass was corrected for the buoyancy by assuming a density of 1.511 g cm^{-3} determined from the X-ray diffraction.[7,8] A small amount of helium gas was sealed in the calorimeter cell to aid heat transfer.

Infrared Absorption Spectroscopy

Infrared spectra were recorded for Nujol mulls at 90, 200, 300 and 330 K in the 4000 –400 cm^{-1} range with an infrared spectrophotometer (Japan Spectroscopic Co., Ltd., Model DS-402G) and far-infrared spectra in the 400 –30 cm^{-1} range with a far-infrared spectrophotometer (Hitachi, Ltd., Model FIS-3). These spectra were used for estimation of the normal heat capacities by use of effective frequency distribution method.[14]

RESULTS

Prior to heat capacity measurements, DTA data were measured for $[Cu(dieten)_2](ClO_4)_2$. The thermogram showed a single endothermic peak at 315 K on heating. A dramatic color change of the compound is easily seen when the sample in a DTA glass tube passes through this temperature on heating or on cooling. Adiabatic calorimetric measurements were made for 10.0294 g of $[Cu(dieten)_2](ClO_4)_2$ in two series: series 1 (12–60 K) and series 2 (44–359 K). The results were evaluated in terms of C_p, the molar heat capacity at constant pressure. The temperature dependence of the observed heat capacities is listed in Table 1 and plotted in Figure 1. As expected from DTA, only a single peak due to the thermochromic phase transition was found at 317.64 K (= T_{trs}). This phase transition is characterized by a long heat-capacity tail extending down to ~200 K, as in the case of $[Cu(dieten)_2](BF_4)_2$.[10] In the vicinity of the phase transition temperature (from 314.71 to 318.30 K), the thermal relaxation time required for the calorimeter cell to reach thermal equilibrium after an energy input was longer than two hours. This long endothermic temperature drift is characteristic of a first-order phase transition.

The observed heat capacity is composed of two parts: one is the normal heat capacity due to the lattice and molecular vibrations and the other is the excess heat capacity arising from the phase transition. In order to separate these two contributions, normal heat capacities were determined independently for the low- and high-temperature phases as follows. The normal heat capacities of the low-temperature phase were estimated by using an effective frequency distribution method.[14] The intramolecular vibration frequencies necessary for this method were collected from the observed infrared spectra and data on related compounds available in the literature. On the other hand, those of the high-temperature phase were estimated by using a polynomial-function fitting. The normal heat capacities estimated by these methods are shown in Figure 1 by dotted curves. They exhibited a gap (= 46 J K^{-1} mol^{-1}) at T_{trs}. Subtraction of the normal heat capacities from the observed values gave the excess heat capacities, ΔC_p, associated with the phase transition. The temperature dependence of the excess heat capacities are shown in Figure 2, in which gradually increasing excess heat capacities with increasing temperature below T_{trs} is clearly seen.

Table 1 Molar heat capacity of $[Cu(dieten)_2](ClO_4)_2$

T / K	C_p / $JK^{-1}mol^{-1}$	T / K	C_p / $JK^{-1}mol^{-1}$	T / K	C_p / $JK^{-1}mol^{-1}$
Series1					
11.797	15.95	25.644	67.31	41.336	124.10
12.568	17.82	26.426	69.54	42.932	129.23
13.545	21.21	27.545	73.72	44.580	134.56
14.510	24.66	28.767	78.38	46.275	139.72
15.517	28.12	30.034	83.12	48.014	144.77
16.611	31.63	31.353	88.27	49.821	150.00
17.829	35.95	32.668	93.41	51.667	155.34
19.077	40.79	33.982	98.43	53.550	160.66
20.240	46.45	35.363	103.44	55.514	166.08
21.441	49.56	36.809	108.64	57.532	171.54
22.721	54.49	38.284	113.84	59.525	176.84
24.009	62.43	39.788	118.97		
Series2					
44.382	133.82	119.027	296.66	203.135	433.91
45.566	137.60	121.126	300.11	205.224	437.24
46.812	141.26	123.205	303.70	207.306	441.28
47.732	143.98	125.277	307.22	209.380	444.79
48.969	147.55	127.345	310.83	211.446	448.19
50.530	152.03	129.396	314.17	213.504	451.76
52.132	156.61	131.429	317.70	215.555	455.21
53.815	161.39	133.447	320.67	217.599	458.73
55.574	166.29	135.448	324.01	219.637	462.62
57.420	171.36	137.436	327.20	221.667	466.30
59.343	176.50	139.409	330.33	223.690	470.04
61.265	181.43	141.404	333.76	225.706	473.92
63.188	186.37	143.443	337.29	227.715	477.49
65.115	191.01	145.492	340.62	229.717	481.39
67.021	195.53	147.527	343.84	231.712	485.11
68.977	199.93	149.549	347.00	233.700	488.67
70.943	204.31	151.559	350.10	235.682	492.30
72.893	208.75	153.557	353.39	237.656	496.35
74.886	213.05	155.543	356.52	239.624	500.33
76.881	217.27	157.552	359.80	241.656	504.26
78.827	221.48	159.608	363.23	243.750	508.09
80.730	225.55	161.675	366.42	245.836	512.28
82.593	229.52	163.754	369.77	247.914	516.90
84.420	233.03	165.852	373.09	249.986	520.91
86.213	236.56	167.946	376.78	252.049	525.38
87.976	240.22	170.029	380.18	254.105	530.30
89.754	243.50	172.101	382.95	256.154	534.88
91.598	247.16	174.163	386.78	258.194	539.57
93.535	250.96	176.253	389.79	260.227	544.62
95.511	254.36	178.315	393.34	262.253	548.89
97.458	257.91	180.366	396.39	264.271	554.23
99.376	261.51	182.408	399.52	266.281	559.85
101.335	265.38	184.441	402.81	268.283	564.99
103.335	268.94	186.465	406.15	270.277	570.21
105.309	272.34	188.481	409.40	272.296	576.88
107.259	275.89	190.488	412.85	274.341	582.27
109.186	279.25	192.559	416.14	276.377	588.95
111.091	282.52	194.692	419.56	278.410	596.29
113.000	285.98	196.815	423.05	280.438	603.03
114.951	289.80	198.930	426.99	282.455	610.25
116.956	293.40	201.037	429.88	284.461	617.68

Table 1 *Continued*

286.457	625.45	315.635	1461.7	327.302	669.44
288.440	634.24	316.121	2288.8	328.705	671.07
290.410	643.07	316.496	3245.8	330.187	672.16
292.366	653.92	316.799	4123.0	331.755	673.73
294.311	662.32	317.056	4984.4	333.410	675.88
296.251	672.45	317.285	5468.6	335.155	677.05
298.180	685.85	317.487	6785.3	337.044	679.22
300.096	697.91	317.644	10108	339.025	681.89
301.996	711.70	317.779	9213.6	341.044	684.60
303.881	727.88	317.941	6805.2	343.058	687.25
305.750	745.92	318.168	4223.2	345.069	689.07
307.599	767.48	318.597	1294.9	347.078	691.69
308.975	784.49	319.264	759.56	349.082	694.71
309.883	800.03	320.027	678.34	351.083	696.29
310.784	816.12	320.902	673.61	353.081	699.62
311.677	833.35	321.898	669.50	355.075	701.76
321.561	856.23	322.920	667.08	357.082	703.84
313.435	884.40	323.942	666.57	359.104	707.00
314.290	935.98	324.963	667.74		
315.037	1068.0	326.058	667.82		

The enthalpy, $\Delta_{trs}H$ (= 17.43 kJ mol^{-1}), and the entropy, $\Delta_{trs}S$ (= 55.21 J K^{-1} mol^{-1}), of transition were determined by integration of ΔC_p with respect to T and ln T, respectively. The temperature dependence of the entropy gain for the phase transition of $[Cu(dieten)_2](ClO_4)_2$ is plotted in Figure 3. The entropy gain consists of two parts: one is the discontinuous part and the other is the gradual part. The discontinuous part occurs just in the temperature region, where the long thermal relaxation time was required for thermal equilibration after an energy input. The gradual part corresponds to the long tail of the excess heat capacity.

DSC measurements have already been carried out by Fabbrizzi *et al.*[6] and they obtained the transition enthalpies as 10.0 kJ mol^{-1} for $[Cu(dieten)_2](BF_4)_2$ and 8.91 kJ mol^{-1} for $[Cu(dieten)_2](ClO_4)_2$. However, the transition enthalpy determined by the adiabatic calorimetry is 16.62[10] and 17.43 kJ mol^{-1} for $[Cu(dieten)_2](BF_4)_2$ and $[Cu(dieten)_2](ClO_4)_2$, respectively. The enthalpies detected by DSC are less than 60 percent of the transition enthalpies. In this type of phase transition, it is usually difficult to accurately obtain the excess enthalpy by DSC, because the transition has a long C_p tail extending below the transition temperature. DSC measurements can sense the discontinuous part but often fail to detect the gradual part.

The standard thermodynamic functions of $[Cu(dieten)_2](ClO_4)$ are listed in Table 2. The effective frequency distribution method[14] was used for the extrapolation below 13 K.

DISCUSSION

Onset of Puckering Motion of the Metal-Ligand Chelate Rings

The crystal structures of $[Cu(dieten)_2](BF_4)_2$ have been determined in both the low- and high-temperature phases.[7,8] They provide a useful clue to the molecular freedom responsible for the entropy gain. The most remarkable change in the

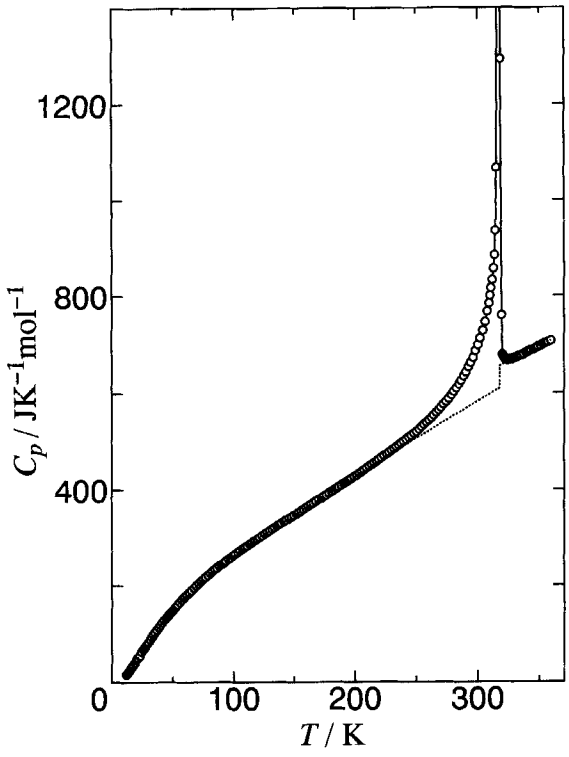

Figure 1 Temperature dependence of the molar heat capacity of $[Cu(dieten)_2](ClO_4)_2$. The dotted curve shows the calculated normal heat capacities. The solid lines are only guides for the eye.

structure occurring through the phase transition is the motion of the chelate rings, which is easily seen from anisotropic thermal ellipsoids of the constituent atoms. The chelate rings are puckering up and down from the CuN_4 plane in the high-temperature phase. Provided that this chelate ring puckering is responsible for an essential part of the transition mechanism, we can estimate the enthalpy gain at the phase transition as follows. Let us assume that the chelate rings are static in the low-temperature phase, whereas they pucker in the high-temperature phase. There are two chelate rings in a cation, consisting of a five-membered CuN_2C_2 ring. When the plane formed by the CuN_2 is fixed, the five-membered ring has four different configurations: two configurations in which two carbon atoms are tipped off to the same side of the plane and two configurations in which two carbon atoms are tipped off to the opposite sides of the plane. It should be remarked that the number of degrees of freedom for the puckering motion of a five-membered ring is two. Moreover, since there exist two chelate rings in a cation, the total number of the puckering modes amounts to four. These four modes are roughly assumed to be degenerate and simply approximated by the Einstein harmonic oscillator. The changes of thermodynamic quantities contributed from one oscillator at the transition point, T_{trs}, are evaluated by means of the following equations:

$$x \equiv \frac{hc\,\tilde{\nu}}{kT_{trs}}, \tag{1}$$

$$\Delta C(x) = R\frac{x^2e^x}{(e^x - 1)^2}, \tag{2}$$

$$\Delta H(x) = RT_{trs}\frac{x}{e^x - 1}, \tag{3}$$

$$\Delta S(x) = R\left\{\frac{x}{e^x - 1} - \ln(1 - e^{-x})\right\}, \tag{4}$$

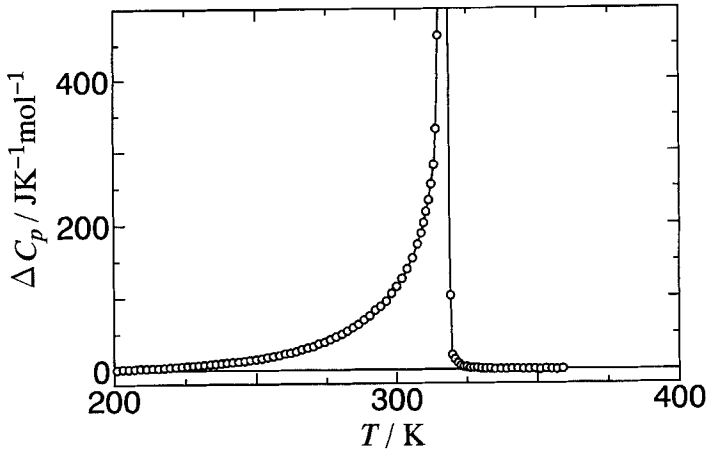

Figure 2 Temperature dependence of the excess heat capacity of $[Cu(dieten)_2](ClO_4)_2$. The solid curves are only guides for the eye.

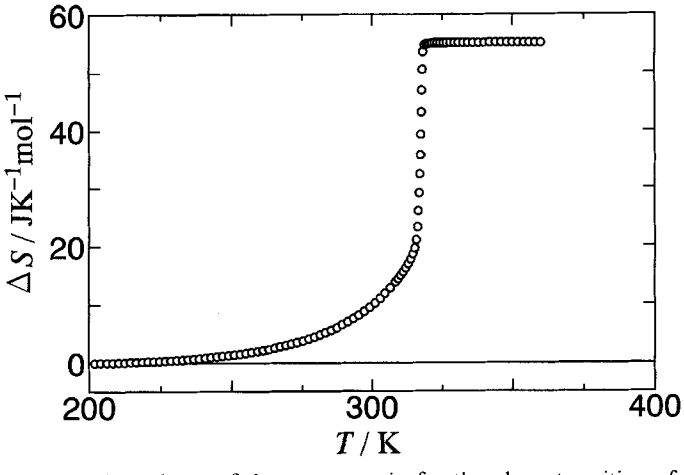

Figure 3 Temperature dependence of the entropy gain for the phase transition of [Cu (dieten)$_2$] $(ClO_4)_2$.

Table 2 Standard thermodynamic functions for $[Cu(dieten)_2](ClO_4)_2$ in the unit of J K^{-1} mol^{-1}; the values in the parentheses are extrapolated

T/K	C_p°	S°	$(H^\circ - H_0^\circ)/T$	$-(G^\circ - H_0^\circ)/T$
5	(1.46)	(0.488)	(0.366)	(0.122)
10	(10.48)	(3.746)	(2.787)	(0.959)
15	26.21	10.832	7.860	2.972
20	45.28	20.809	14.689	6.120
30	82.99	46.343	31.226	15.117
40	119.68	75.390	48.888	26.502
50	150.52	105.507	66.228	39.280
60	178.09	135.436	82.609	52.826
70	202.21	164.765	98.024	66.741
80	223.98	193.203	112.427	80.775
90	243.99	220.761	125.960	94.801
100	262.74	247.448	138.707	108.742
110	280.65	273.345	150.808	122.538
120	298.26	298.538	162.378	136.160
130	315.22	323.081	173.487	149.593
140	331.34	347.031	184.186	162.845
150	347.70	370.462	194.556	175.906
160	363.83	393.412	204.627	188.785
170	380.13	415.951	214.465	201.486
180	395.85	438.119	224.100	214.019
190	412.01	459.946	233.556	226.390
200	428.46	481.498	242.886	238.612
210	445.81	502.817	252.134	250.683
220	463.27	523.950	261.326	262.624
230	481.92	544.951	270.509	274.442
240	501.06	565.856	279.706	286.150
250	520.94	586.707	288.953	297.754
260	544.06	607.581	298.311	309.269
270	569.48	628.576	307.869	320.706
280	601.57	649.848	317.768	332.081
290	641.23	671.613	328.201	343.412
300	697.31	694.238	339.513	354.725
310	802.12	718.547	352.482	366.065
		Phase transition at 317.64 K		
320	681.22	778.412	401.886	376.526
330	672.03	799.019	410.002	389.017
340	683.20	819.237	417.862	401.375
350	695.43	839.219	425.620	413.600
273.15	579.13	635.238	310.941	324.297
298.15	685.64	689.960	337.329	352.632

where h, c, k and R are the Planck constant, the speed of light, the Boltzmann constant and the gas constant, respectively. $\tilde{\nu}$ is a wave number of the puckering motion. If we assume that this puckering motion is responsible for the total entropy of transition, then $\tilde{\nu}$ is calculated to be 115 cm^{-1} for $[Cu(dieten)_2](ClO_4)_2$ and 109 cm^{-1} for $[Cu(dieten)_2](BF_4)_2$ from the relation, $4\Delta S(x) = \Delta_{trs}S$. $\Delta_{trs}H$ and ΔC_p are similarly obtained from $4\Delta H(x)$ and $4\Delta C(x)$, respectively. The estimated values from the chelate ring puckering motion are listed in Table 3. $4\Delta C(x)$ corresponds to a heat-capacity gap between two base lines at T_{trs}. The calculated gap, 33 J K^{-1} mol^{-1} is nearly equal to the average value of the experimental data for the two

Table 3 Comparison of the theoretical and observed quantities. T_{trs}, $\Delta_{trs}H$ and $\Delta_{trs}S$ are observed transition temperature, enthalpy and entropy of transition, respectively. $\Delta H(x)$ and $\Delta C(x)$ are calculated by equations (1) – (4), where $x \equiv hc\tilde{\nu}/kT_{trs}$. ΔC_p indicates the gap of the normal heat capacities at T_{trs}. ΔH(AOM) is the enthalpy gain due to the change in the *d*-electronic state. ΔH(total) is the sum of $4\Delta H(x)$ and ΔH(AOM).

Complex	T_{trs}	$\Delta_{trs}H$	$\Delta_{trs}S$	ΔC_p	$4\Delta C(x)$	$4\Delta H(x)$	ΔH(AOM)	ΔH(total)
	K	kJ mol^{-1}	J K^{-1} mol^{-1}	J K^{-1} mol^{-1}	J K^{-1} mol^{-1}	kJ mol^{-1}	kJ mol^{-1}	kJ mol^{-1}
$[Cu(dieten)_2](BF_4)_2$	302.64	16.62	55.3	16	33	7.7	9.1	16.8
$[Cu(dieten)_2](ClO_4)_2$	317.64	17.43	55.2	46	33	8.0	8.4	16.4

complexes, about 31 J K^{-1} mol^{-1}. The contribution of the chelate ring puckering to the observed $\Delta_{trs}H$ is about 46% for each complex.

Electronic Energy Derived from the Angular Overlap Model (AOM)

According to the X-ray structural analysis of $[Cu(dieten)_2](ClO_4)_2$,[7,8] there is no significant change in the Cu-N distances, whereas the *trans* bond angles of N-Cu-N change slightly through the phase transition. In the low-temperature phase the angles are 180.0°, while in the high-temperature phase they are 178.0° and 174.7°. The $[Cu(dieten)_2]^{2+}$ cation is characterized by a square-planar coordination geometry in the low-temperature phase. This geometry is slightly distorted toward a tetrahedral coordination in the high-temperature phase. Despite such a small geometrical change, the color of complexes changes dramatically when the phase transition occurs. The color of the complexes depends obviously on the absorption of visible light by a molecule. The absorption spectra in the visible region depend on the energy-level splitting of the *d*-orbitals. Variable-temperature *d-d* transition of $[M(dieten)_2]X_2$ has already been studied.[4–6] These complexes show a red shift in the *d-d* transition when they are heated. To investigate the relationship between the absorption spectra and the *d*-orbital energy levels, the angular overlap model (AOM)[15–18] was adopted. In this model, the interactions between the *d*-orbitals of the central metal and the ligand orbitals are estimated on the basis of the coordination geometry. The relative energy levels of the *d*-orbitals are calculated by solving the secular determinant which consists of the following matrix elements, E_{ij} $(i, j = 1 \cdots 5)$.

$$E_{ij} = e_\sigma \sum_{n=1}^{4} F(d_i, L_n)F(d_j, L_n), \tag{5}$$

where e_σ is an energy unit describing a σ-type interaction and $F(d, L)$ indicates the angular overlap factors for the *d*-orbitals of the central metal atom and the ligand orbitals. Many ligands such as NH_3 are known to have very little π-bonding to metal ions. Then only the σ-type interactions are treated in this model. The angular dependences of these factors are given in Table 4. There are two types of N atoms in the present complexes: one is bonded to two ethyl-group while the other has no ethyl moieties. Consequently there exist small differences in the Cu-N bond lengths. If this fact is taken into account, the symmetry of the CuN_4 plane becomes D_{2h}. On the other hand, if this difference is negligibly small, the symmetry of the CuN_4 plane is approximated by D_{4h}. The primary effect of lowering the symmetry from D_{4h} to D_{2h} is to lift the degeneracy of the two levels, d_{xz} and d_{yz}. Since this splitting is

expected to be small,[19] four nitrogen atoms are treated to be equal for the sake of simplicity of the evolution of the matrix elements given by equation (5).

The structure of $[Cu(dieten)_2]^{2+}$ changes from a square-planar configuration in the low-temperature phase to a slightly tetrahedrally-distorted coordination in the high-temperature phase. The relative energies of the five *d*-orbitals can be calculated as a function of the polar angles (θ, ϕ) of the ligand position vectors. The central metal atom and the ligand nitrogen atoms are arranged in the polar coordinate system. In the case of square-planar geometry (D_{4h}), four nitrogen atoms are put on the positions $L_1(90°, 0°)$, $L_2(90°, 90°)$, $L_3(90°, 180°)$ and $L_4(90°, 270°)$, while in the case of tetrahedral geometry (T_d), they are put on the positions $L_1(54.74°, 45°)$, $L_2(125.26°, 135°)$, $L_3(54.74°, 225°)$ and $L_4(125.26°, 315°)$. In between these two coordination geometries, the positions of ligand nitrogens are given as follows: $L_1(\theta, \phi)$, $L_2(180° - \theta, \phi + 90°)$, $L_3(\theta, \phi + 180°)$ and $L_4(180° - \theta, \phi + 270°)$, where θ is variable in the 90°–54.74° range and ϕ is in the 0°–45° range. The relative energies of the *d*-orbitals are calculated from these parameters (θ, ϕ) and the angular overlap factors (F) given in Table 4. The calculated energy levels are illustrated in Figure 4 as a function of θ. The unit of the ordinate axis, e_σ, corresponds to $\Delta E(90)/3$. Temperature effects on the electronic spectrum of $[M(dieten)_2]X_2$ have been reported.[4,5] The visible light absorption maximum is shifted from 20750 cm^{-1} in the low-temperature phase to 19230 cm^{-1} in the high-temperature phase for $[Cu(dieten)_2](BF_4)_2$, while from 20700 cm^{-1} to 19305 cm^{-1} for $[Cu(dieten)_2](ClO_4)_2$. The absorption maximum in the electronic spectrum corresponds to the d_{yz}, $d_{xz} \rightarrow d_{x^2-y^2}$ transition. Namely, the transition energy, $hc\,\tilde{\nu}_{max}$, is the energy difference between these two orbitals, $\Delta E(\theta)$ in Figure 4. In the low-temperature phase, since the coordination geometry is D_{4h}, $\Delta E(90)$ is equal to $hc\,\tilde{\nu}_{max}$ observed at lower temperature, while in the high-temperature phase $\Delta E(\theta)$ is equal to $hc\,\tilde{\nu}_{max}$ recorded at higher temperature. Therefore, the following relation is obtained,

$$\frac{\Delta E(90)}{\Delta E(\theta)} = \frac{hc\,\tilde{\nu}_{max} \text{ at lower temp.}}{hc\,\tilde{\nu}_{max} \text{ at higher temp.}} \qquad (6)$$

The *trans* bond angle, $\angle$ N–Cu–N = 2θ, is estimated from $\Delta E(\theta)$ in this equation and the observed $hc\,\tilde{\nu}_{max}$ values.

The enthalpy (actually the internal energy) or the *d*-orbitals is the sum of each electron's energy. The *d*-electrons are accommodated in the energy level diagram shown in Figure 4, one by one from bottom to top. There are nine *d*-electrons in

Table 4 The angular overlap factors of the *d*-orbitals of a central atom as a function of the ligand position in polar coordinate, (θ, ϕ), with a ligand σ-type orbital.

d-orbital	$F(d, L(\theta, \phi))$
d_{z^2}	$(1 + 3\cos 2\theta)/4$
d_{yz}	$\sqrt{3}\sin\phi \sin 2\theta/2$
d_{xz}	$\sqrt{3}\cos\phi \sin 2\theta/2$
d_{xy}	$\sqrt{3}\sin 2\phi\,(1 - \cos 2\theta)/4$
$d_{x^2-y^2}$	$\sqrt{3}\cos 2\phi\,(1 - \cos 2\theta)/4$

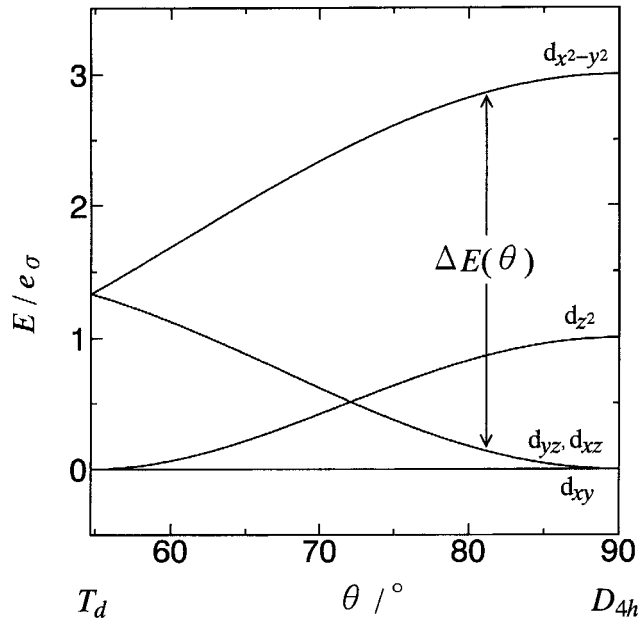

Figure 4 Energy level diagram calculated on the basis of the angular overlap model.

the copper complexes. The enthalpy of the *d*-orbitals in the low-temperature phase is calculated from the energy-scheme at $\theta = 90°$, whereas that in the high-temperature phase is calculated from the scheme at the θ estimated from equation (6). Consequently, the enthalpy change of the *d*-orbitals arising from the change in the coordination geometry is straightforwardly determined as the difference between the electron energies of the low- and high-temperature phases. The *trans* bond angle, ∠N–Cu–N, of $[Cu(dieten)_2](ClO_4)_2$ in the high-temperature phase estimated from AOM is 164.4°, while the X-ray structural analyses[7,8] have indicated 178.0° and 174.7°. A small disagreement of the bond angle between experiment and theory likely reflects the approximate nature of the AOM. In the case of $[Cu(dieten)_2](BF_4)_2$, the calculated bond angle is 165.0°, however an X-ray structural analysis has not been carried out.

The contribution of the *d*-orbital energy of the transition enthalpy is 9.1 and 8.4 kJ mol^{-1} for $[Cu(dieten)_2](BF_4)_2$ and $[Cu(dieten)_2](ClO_{4_2}$, respectively. These contributions amount to 54 and 48% of the respective observed enthalpy gain at the phase transition.

Enthalpy Gain at the Phase Transition

Thermodynamic investigations of phase transition phenomena are often described in terms of an "entropy" gain at a given phase transition. This physical quantity surely plays a diagnostic role for inspection of the nature of phase transitions, because the entropy, though a macroscopic quantity, is correlated with the randomness or disorder occurring on microscopic levels by means of the Boltzmann

principle. However, if we take into account the fact that thermodynamic stability between two phases is determined by the free energy difference, $\Delta G = \Delta H - T\Delta S$, it is clear that an "enthalpy" gain at the phase transition also plays an important role. The transition enthalpy provides us with information concerning the interaction energy involved in the phase transition. For example, even if the transition entropy is identical between two substances, the transition temperature may primarily be varied according to the enthalpy gain: the stronger the interaction energy, the higher the transition temperature.

We have so far regarded the observed transition enthalpy, $\Delta_{trs}H$, as consisting of two contributions: one is the enthalpy gain due to the onset of the puckering motion of the metal-ligand chelate rings and the other is the electronic energy gained by a change in the coordination geometry across the phase transition. These two contributions were analyzed in terms of the harmonic oscillator model and the angular overlap model, respectively. As summarized in Table 3, the former is $4\Delta H(x) = 8.0$ kJ mol^{-1} for $[Cu(dieten)_2](ClO_4)_2$, where $x = hc\tilde{\nu}/kT_{trs}$, and the latter amounts to $\Delta H(\text{AOM}) = 8.4$ kJ mol^{-1}. The sum of these contributions corresponds to the theoretical enthalpy gain, $\Delta H(\text{total}) = 16.4$ kJ mol^{-1}. Surprisingly this theoretical value well accounts for the observed value, $\Delta_{trs}H = 17.43$ kJ mol^{-1}. Finally, an even better agreement has been attained for $[Cu(dieten)_2](BF_4)_2$, in which $\Delta_{trs}H$ and $\Delta H(\text{total})$ are 16.62 and 16.8 kJ mol^{-1}, respectively.

Entropy Gain at the Phase Transition

Although the themochromic phase transition of $[Cu(dieten)_2](ClO_4)_2$ occurs at 317.64 K, which is 15 K higher than that of $[Cu(dieten)_2](BF_4)_2$, their transition entropies are essentially equal: 55.2 and 55.3 J K^{-1} mol^{-1} for the ClO_4^- and BF_4^- salts, respectively. This indicates that the degrees of molecular freedom that are excited when the thermochromic phase transition takes place are identical for both complexes. In other words, the mechanism responsible for the thermochromism of one complex is similar to that of the other complex.

In the case of the enthalpy gain, both contributions from the puckering motion and the electronic energy due to the geometrical change were taken into account. However, we regarded the transition entropy as arising only from the onset of puckering motion of the metal-ligand chelate rings at the phase transition temperature. By equating the observed entropy gain, $\Delta_{trs}S$, to the puckering entropy, $4\Delta S(x)$, we estimated the characteristic frequency of the puckering motion in terms of the wave number, $\tilde{\nu}$. On the basis of this characteristic frequency, we determined a heat-capacity gap at the transition temperature between the low- and high-temperature phases, as well as the enthalpy gain due to the puckering motion. The estimated heat-capacity gap at T_{trs} accounts fairly well for the experimental value and, moreover, the observed transition enthalpy agrees well with the sum of the enthalpy gains arising from the puckering motion and the electronic energy. Based on this fact, we can expect that the entropy gain due to the change in the electronic state might be very small for the present series of complexes.

Mechanisms of Thermochromic Phase Transitions

Various mechanisms have been reported to be responsible for thermochromic phenomena occurring in the solid state.[1,2] In the case of spin-crossover complexes, a

dramatic change in their color occurs by virtue of a discontinuous change in the metal-ligand distances while maintaining the coordination geometry around a central metal atom. The large entropy difference between the high- and low-spin states, necessary for the Gibbs free-energy crossing, mainly originates in phonon entropy gained by softening of the metal-ligand skeletal vibrational modes on going from the low- to high-spin state.[20–22]

Another typical example of thermochromic compounds is tetra-coordinated Ni(II) complexes: isomerism between the square-planar diamagnetic green form and the tetrahedral paramagnetic brown form.[23,24] In this case a drastic configurational change is responsible for the thermochromism and the entropy difference is based on a different distribution of normal mode and lattice vibrations.

In the case of $(IPA)CuCl_3$[25] and $(IPA)_2CuCl_4$,[25] where IPA is isopropylammonium ion, the color changes are caused by a change in the coordination number. Since such a change is very drastic, the potential barrier hindering interconversion between the conformation characteristic of the low-temperature phase and that of the high-temperature phase would be extremely high. This seems to be the reason for the remarkable super-heating effect of the low-temperature phase and undercooling effect of the high-temperature phase.

In the present $[Cu(dieten)_2]X_2$ ($X = ClO_4^-$ or BF_4^-) complexes dynamic interconversion between ligand conformations plays a fundamental role in the mechanism of thermochromic phase transitions and configurational entropy mainly contributes to the entropy gain. A very similar situation has been encountered in the thermochromic complex $[Cu(daco)_2](NO_3)_2$, where daco = 1,5-diazacyclooctane.[26] Each eight-membered daco ring statically coordinates to the central copper ion with a fixed chair-boat conformation in the low-temperature phase, whereas dynamic interconversion between the chair and the boat from takes place in the high-temperature phase. The entropy gain is well accounted for in terms of conformational disordering of the daco ligand.

Therefore, the present complexes $[(Cu(dieten)_2]X_2$, together with $[Cu(daco)_2](NO_3)_2$, form a new class of thermochromic family, in which dynamic motion of the ligands is responsible for the mechanism of thermochromism. Calorimetric studies on the homologous complexes $[Ni(dieten)_2]X_2$ ($X = ClO_4^-$ or BF_4^-) are presently being undertaken.

Acknowledgement

This study was partially supported by the NSF grant CHE-9115286 (D.N.H).

References

1. K. Sone and Y. Fukuda, *Inorganic Thermochromism* (Inorganic Chemistry Concepts, Vol. 10, Springer-Verlag, Berlin, 1987).
2. D.B. Bloomquist and R.D. Willett, *Coord. Chem. Rev.* **47**, 125 (1982).
3. P. Pfeiffer and H. Glaser, *J. Prakt. Chem.***151**, 134 (1938).
4. J.R. Ferraro, L.J. Basile, L.R. Gracia-Ineguez, P. Paoletti and L. Fabbrizzi, *Inorg. Chem.* **15**, 2342 (1976).
5. A.B.P. Lever, E. Mantovani and J.C. Donini, *Inorg. Chem.* **10**. 2424 (1971).
6. L. Fabbrizzi, M. Micheloni and P. Paoletti, *Inorg. Chem.* **13**, 3019 (1974).
7. M.M. Andino, J.D. Curet and M. M. Muir, *Acta Crystallogr.* **B32**, 3185 (1976).

8. I. Grenthe, P. Paoletti, M. Sandström and S. Glikberg, *Inorg. Chem.* **18**, 2687 (1979).
9. R.J. Pylkki, R.D. Willett and H.W. Dodgen, *Inorg. Chem.* **23**, 594 (1984).
10. A. Nishimori, E.A. Schmitt, D.N. Hendrickson and M. Sorai, *J. Phys. Chem. Solids* **55**, 99 (1984).
11. D.B. Chesnut, *J. Chem. Phys.* **40**, 405 (1964).
12. M. Yoshikawa, M Sorai, H. Suga and S. Seki, *J. Phys. Chem. Solids* **44**, 311 (1983).
13. A. Nishimori, Y. Nagano and M. Sorai, unpublished result.
14. M. Sorai and S. Seki, *J. Phys. Soc. Jpn* **32**, 382 (1972).
15. J.K. Burdett, *Adv. Inorg. Chem. Radiochem.* **21**, 113 (1978).
16. E. Larsen and G.N. La Mar, *J. Chem. Educ.* **51**, 633 (1974).
17. W. Smith and D.W. Clark, *Rev. Roum. Chim.* **20**, 1243 (1975).
18. A.B.P. Lever, *Inorganic Electronic Spectroscopy* (second edition) (Studies in Physical and Theoretical Chemsitry, Vol. 33, Elsevier, Amsterdam, 1984).
19. K.L. Bray, H.G. Drickamer, E.A. Schmitt and D.N. Hendrickson, *J. Am. Chem. Soc.* **111**, 2849 (1989).
20. M. Sorai and S. Seki, *J. Phys. Soc. Jpn* **33**, 575 (1972); *J. Phys. Chem. Solids* **35**, 555 (1974).
21. K. Kaji and M. Sorai, *Thermochim. Acta* **88**, 185 (1985).
22. M. Sorai, Y. Yumoto, D.M. Halepoto and L.F. Larkworthy, *J. Phys. Chem. Solids* **54**, 421 (1993).
23. A. Takeuchi and S. Yamada, *Bull. Chem. Soc. Jpn* **42**, 3046 (1969).
24. N. Arai, M. Sorai and S. Seki, *Bull. Chem. Soc. Jpn* **45**, 2398 (1972).
25. A. Nishimori and M. Sorai, unpublished result.
26. H. Hara and M. Sorai, *J. Phys. Chem. Solids* **56**, 223 (1995).